PHYSICAL REVIEW B **84**, 035211 (2011)

Vibrational modes and lattice distortion of a nitrogen-vacancy center in diamond from first-principles calculations

Jianhua Zhang,[1,2] Cai-Zhuang Wang,[1] Z. Z. Zhu,[2] and V. V. Dobrovitski[1]
[1]*Ames Laboratory, Iowa State University, Ames, Iowa 50011, USA*
[2]*Department of Physics and Institute of Theoretical Physics and Astrophysics, Xiamen University, Xiamen 361005, China*
(Received 18 March 2011; revised manuscript received 10 June 2011; published 29 July 2011)

We investigate vibrational properties and lattice distortion of negatively charged nitrogen-vacancy (NV^-) center in diamond. Using the first-principles electronic structure calculations, we show that the presence of NV^- center leads to appearance of a large number of quasilocalized vibrational modes (qLVMs) with different degrees of localization. The vibration patterns and the symmetries of the qLVMs are presented and analyzed in detail for both ground and excited orbital states of the NV^- center. We find that in the high-symmetry (C_{3v}) excited orbital state a pair of degenerate qLVMs becomes unstable, i.e., has formally negative frequencies, and the stable excited state has lower (C_{1h}) symmetry. This is a direct indication of the Jahn-Teller effect, and our studies suggest that the dynamical Jahn-Teller effect in the weak-coupling regime takes place. We have also performed a detailed comparison of our results with the available experimental data on the vibrations involved in optical emission/absorption of the NV^- centers. We have directly demonstrated that, among other modes, the qLVMs crucially impact the optical properties of the NV^- centers in diamond, and identified the most important groups of qLVMs. Our results are important for deeper understanding of the optical properties and the orbital relaxation associated with lattice vibrations of the NV^- centers.

DOI: 10.1103/PhysRevB.84.035211 PACS number(s): 71.55.−i, 71.15.Mb, 63.20.Pw, 78.55.−m

I. INTRODUCTION

The negatively charged nitrogen-vacancy (NV^-) impurity centers in diamond have attracted much interest in recent years. They demonstrate a uniquely favorable combination of spin and optical properties: a NV^- electronic spin has long coherence time,[1–4] the spin state of a single NV^- center can be optically initialized and read out,[5,6] and can be manipulated both optically[7–9] and magnetically.[10,11] As a result, NV^- centers constitute promising candidates for applications in quantum information processing,[12–14] high-sensitivity magnetometry with nanoscale resolution,[15–17] and photonics.[18–22] The NV^- centers also present an excellent platform for studying such fundamental problems of quantum mechanics as the dynamics of quantum spins coupled to their environment,[1,2,23–25] and for exploring quantum control and dynamical decoupling of solid-state spins.[11,23–26]

The electronic, optical, and spin properties of the NV^- centers are strongly affected by the lattice vibrations. For instance, due to slightly different atomic arrangement in the ground state and the excited state of the NV^- center, the optical emission and absorption is accompanied by the lattice motion, i.e., involves the vibrational lattice excitation.[27–29] The impact of lattice motion on the properties of the NV^- centers has been under investigation from the 1970s[30,31] until now.[26,32–34] The lattice vibrations are responsible for the broadening of the light emission spectrum and appearance of additional spectral features,[30,31] for depolarization of the emitted photons,[21,31,33] and for the orbital and spin relaxation of the NV^- centers.[26,32–34] The localized and quasilocalized vibrational modes are especially important for defect centers in semiconductors, and are often used for investigation of their properties.[35–38] The detailed studies of the lattice vibrations, and of the (quasi)localized modes in particular, would be very useful for deeper understanding of the optical properties of NV^- centers, and would greatly improve our knowledge of the phonon-assisted spin and orbital relaxation of this system. Such studies are also useful for improvement of the optical properties of NV^- centers, as required for photonic-related applications.[8,18–22] Very recently, a first study of several localized modes has been reported for the NV^- center.[39] But detailed studies of other numerous localized and quasilocalized modes, which could be important for better understanding of the experimental data,[30,31] are still lacking.

In this paper, we present a detailed first-principles study of the localized distortions and vibrational properties of the negatively charged NV^- centers in diamond in its ground and excited orbital states. We show that the presence of the NV^- impurity noticeably modifies the vibrational spectrum, and leads to the appearance of numerous quasilocalized vibrational modes (qLVMs) with different degrees of localization. We present a detailed description of several important qLVMs, and analyze the changes in these modes upon optical excitation. Comparing our results with earlier experiments,[30,31] we show that qLVMs crucially influence the luminescence properties of the NV^- centers. The partial density of states (DOS) of the vibrations (quasi)localized on the NV^- center is in excellent quantitative agreement with the results of Ref. 30. This is the first, to our knowledge, first-principles explanation of these experiments. Our results also suggest that the one-phonon sidebands in the NV^- center emission and absorption spectra are controlled by qLVM. We give a detailed description of the relevant modes, and show that their properties (symmetry and energy) are in agreement with the experimental results.[31]

Another interesting finding reported here is that some of the localized vibrational modes are unstable, i.e., have formally negative frequencies, for the high-symmetry (C_{3v}) excited orbital state of the NV^- center. This is a direct indication that the Jahn-Teller (JT) effect influences the excited state, either by lowering the symmetry of the system (static JT

effect), or by entangling vibrational and electronic states (dynamic JT effect). Our calculations, as well as the known experimental facts, evidence the latter. According to our results, the frequencies of the relevant modes are much larger than the JT energy, indicating the regime of the weak vibronic coupling, in agreement with known facts (such as, e.g., small renormalization of the g factor and the shape of the optical transition bands). However, detailed quantitative theory of the JT effect in NV^- centers requires a separate focused investigation, which is to be performed in the future.

The rest of the paper is organized as follows. In Sec. II we describe the computational method used in the paper. In Sec. III we give a detailed description of the electronic structure of the negatively charged NV^- color center, and optimization of the atomic geometry. We discuss the local distortion of the atomic configuration in the ground and the excited states, and discuss the possibility of the static and dynamic JT effects in the excited state. In Sec. IV we present the results for the lattice vibrations in the ground and in the excited state. We discuss the phonon DOS, localization of different modes, and their properties. In Sec. V, we perform and extensive comparison of our results with the known experimental data. Conclusions are given in Sec. VI.

II. COMPUTATIONAL METHOD

The first-principles calculations were performed within the density-functional theory (DFT) under the generalized gradient approximation (GGA) of Perdew, Burke, and Ernzerhof (PBE),[40] including spin polarization. The Vienna Ab-initio Simulation Package (VASP)[41] has been used to perform geometry optimization and force calculations. A single electron was added to the electron occupancy for the negatively charged vacancy. The extra electron is balanced by a uniform positive background to ensure that the overall supercell is electrically neutral. We used the Γ point for k-point sampling and a plane-wave basis set with a cutoff of 420 eV.

The atomic structures of the NV^- center in its electronic ground and excited states have been optimized before the calculations for the vibration modes are performed. In the geometry optimization calculations, a 215-atom ($3 \times 3 \times 3$) cubic supercell with the box length of $3a_0 = 10.719$ Å was used, where a_0 is the lattice constant of the diamond structure optimized by the VASP calculation. All internal atomic positions were relaxed until the forces were smaller than 10^{-3} eV/Å.

The vibrational modes for the ground state and excited state of the NV^- center were calculated within the harmonic approximation by first-principles calculations. The force-constant matrix of the supercell containing a negatively charged NV^- center defect is evaluated through the forces calculated via the Hellmann-Feynman theorem when each atom in the supercell is displaced one by one from its equilibrium position along $\pm x$, $\pm y$, and $\pm z$ directions, respectively, with a small displacement.[42] We chose a displacement amplitude of 0.02 Å from the atomic equilibrium positions in three Cartesian directions in the force calculation. The amplitude (0.02 Å) is chosen here because it is small enough to remain in the harmonic part of the potential but large enough to avoid numerical noise. The forces acting on all other atoms within the supercell due to the one-by-one displacements of the atoms are used to construct the force-constant matrix of the system. The 642 phonon frequencies plus three translational modes and their corresponding eigenvectors are obtained by diagonalizing the 645×645 force-constant matrix.

III. ELECTRONIC STRUCTURE OF THE NV^- CENTER AND LOCAL DISTORTIONS FROM FIRST-PRINCIPLES GEOMETRY OPTIMIZATION

The nitrogen-vacancy (NV^-) color center consists of a substitutional nitrogen atom (N) and an adjacent vacancy (V) in the diamond lattice. The main features of its atomic and electronic structure are known rather well, and have been recently reviewed in detail in Ref. 43. For a negatively charged NV^- center, the six excess electrons are localized around the center. In the orbital ground state, the atomic arrangement has C_{3v} point symmetry, where one of the $\langle 111 \rangle$ crystallographic axes (passing through the N atom and the vacancy site) is the symmetry axis. Our calculations of the relaxed atomic structure are in agreement with these facts; see Fig. 1. The N and C atoms at the nearest-neighbor shell of the vacancy relax outwards from vacancy. The atomic displacements from initial unrelaxed structure for the N and C atoms are 0.148 and 0.101 Å, respectively, and the distances from the vacancy to nitrogen and carbon atoms in the relaxed structure are 1.695 and 1.646 Å, respectively. These results agree with those obtained previously; see, e.g., Refs. 44–47.

The C_{3v} point group has two types of nondegenerate singlet representations (A_1 and A_2), and a doubly degenerate representation E; below we will use lower-case letters to denote representations for single-electron states and vibration modes, and upper-case letters for many-electron states. The many-electron ground state of a NV^- center is an orbital singlet with the total electron spin $S = 1$, corresponding to

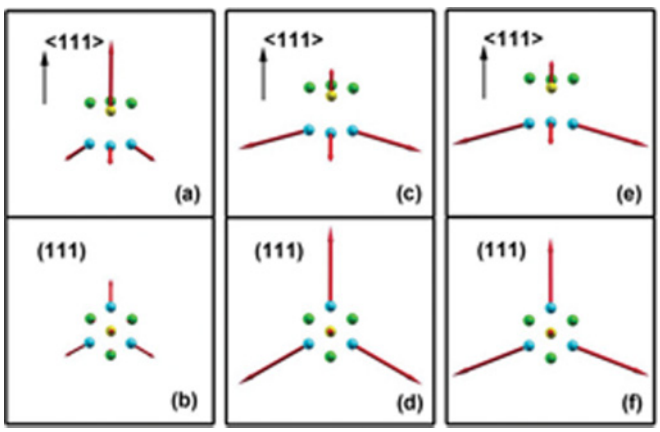

FIG. 1. (Color online) Atomic displacements after geometry optimization, side view (top panels) and top view (bottom panels), with respect to the $\langle 111 \rangle$ axis. The red arrows show the atomic displacements, the arrow length is proportional to the displacement magnitude. (a),(b) ground state, C_{3v} symmetry; (c),(d) excited ^3E state with C_{3v} symmetry; (e),(f) the same excited state, but fully relaxed, with C_{1h} symmetry. Yellow spheres denote N atom, blue spheres denote the C atoms adjacent to the vacancy, green spheres denote the C atoms adjacent to the N atom.

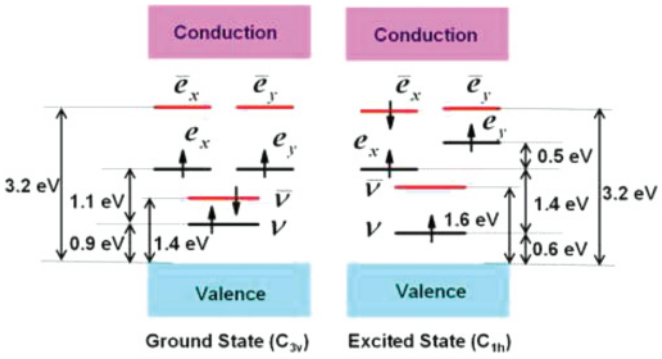

FIG. 2. (Color online) The single-electron orbitals in the ground $^3A_2$ and excited ^3E orbital states of the negatively charged NV^- center. The energies are given with respect to the top of the valence band. The states within the valence band are not shown. The symbols with the bar denote the spin-down states, the symbols without the bar correspond to the spin-up states. The states ν and $\bar{\nu}$ have a_1 symmetry, all other states have e symmetry. We use the notations of the parent C_{3v} group to classify the states of the excited state with C_{1h} symmetry, in spite of the reduced symmetry of the latter.

$^3A_2$ representation (spin triplet, orbital singlet of A_2 type). This state can be visualized within the qualitative model[43] where six electrons localized at the NV^- center populate the single-electron spin-resolved orbitals,[43,48] as shown in Fig. 2. Two electrons occupy the spin-up and spin-down levels immersed in the valence band; we exclude them from consideration. The next two electrons occupy the states ν and $\bar{\nu}$ (spin up and spin down, respectively) of a_1 symmetry. These orbitals are in the band gap of the bulk diamond, and are localized at the carbons surrounding the vacancy and near the nitrogen. The two remaining electrons occupy two degenerate spin-up orbitals of e symmetry (e_x and e_y); the corresponding spin-down orbitals are unoccupied. The energies of the single-electron states calculated here are in agreement with the previously published results.[44–46,49]

Upon optical excitation the NV^- center undergoes transition to an excited state of ^3E symmetry (spin triplet, orbital doublet), which can be qualitatively visualized as a transition of an electron from $\bar{\nu}$ to one of the spin-down orbitals $\bar{e}_x$ or $\bar{e}_y$. Starting from the optimized C_{3v} geometry of the ground state, we found that the system conserves this symmetry after geometry optimization in the excited state. The outward atomic displacements of the N and C atoms are 0.090 and 0.156 Å, respectively; see Fig. 1 (middle panel), and the resulting C-to-vacancy and N-to-vacancy distances are 1.68 and 1.63 Å, respectively, also consistent with previous work.[44]

However, if the geometry optimization for the excited state starts from a low-symmetry atomic arrangement, then the fully relaxed structure has the symmetry of the point group C_{1h}. The signs of an instability of the C_{3v} configuration are seen in the phonon spectrum: the high-symmetry C_{3v} excited state possesses two degenerate soft unstable phonon modes with formally negative frequencies. Thus the total energy surface in the vicinity of the high-symmetry C_{3v} configuration has a saddlelike shape in the multidimensional space. Along most directions (corresponding to stable phonon modes), the curvature of the total-energy surface is positive, while several directions (which correspond to the unstable modes) exhibit very large negative curvature. In contrast, in the vicinity of the low-symmetry C_{1h} configuration, the potential-energy surface has positive curvature along all directions. The energy of the C_{1h} atomic configuration is 6.4 meV lower than the energy of the high-symmetry C_{3v} configuration. While the displacements of the N atom in the C_{1h} and C_{3v} configurations are the same, the displacements of the carbons adjacent to the vacancy are different: one moves by 0.147 Å away from the vacancy site, and the two others move by 0.158 Å see Fig. 1. To check the possible finite-size effect in the geometry relaxation, we repeated this calculation for a twice larger supercell, with 511 atoms. The same result has been obtained, with the fully relaxed structure in the excited orbital state having C_{1h} symmetry, and the energy difference with the C_{3v} configuration was 7.7 meV. The slightly larger energy difference for bigger supercell is expected, since more atoms around the defect can be relaxed. Note that the unstable modes have not been found in the recent calculations,[39] either due to a different calculation method, or due to a smaller size of the supercell used there.

This symmetry breaking is not very surprising. The structure of the excited state corresponds to the typical case where the Jahn-Teller (JT) effect arises:[50–52] the system of C_{3v} symmetry with two degenerate E-type electronic states and two degenerate e-type phonon modes ($E \otimes e$ case). In agreement with expectations, the energy difference between the parent high-symmetry C_{3v} configuration and the symmetry-broken C_{1h} structure comes mainly from the asymmetric relaxation of the atoms adjacent to the vacancy. Therefore although the magnitude of the energy difference does not noticeably exceed the error of the DFT-PBE calculations, we expect that the C_{1h} configuration is indeed the lowest-energy configuration at zero temperature *within adiabatic approximation*. This corresponds to the static JT distortion of the NV^- center's atomic structure, when the energy of the system has three potential-energy minima, related to each other via rotation by the angle $2\pi/3$ around the symmetry axis of the parent C_{3v} structure. At higher temperatures, exceeding the C_{3v}-C_{1h} energy difference (above ~100 K), all energy minima would be occupied equally, and an effective C_{3v} symmetry would be observed in most (but not all) experimental situations.[50]

There is another possibility for the original C_{3v} symmetry to be restored, the dynamical JT effect. Our calculations have been performed within the adiabatic approximation, where the atoms are treated as classical point objects with well-defined coordinates. This approximation may become invalid when two electron states are degenerate, as is the case for the C_{3v} excited state.[50] The atomic motion then should be treated quantum mechanically, and the vibrations may become strongly entangled with orbital degrees of freedom. When the JT energy barrier E_{JT} is much lower than the relevant vibrational frequencies ω, the relief of the potential-energy surface is negligible in comparison with the zero-point atomic vibrations, and the total symmetry of the coupled electron-lattice system is C_{3v} even at zero temperature. Recent experimental evidence is in favor of the dynamical JT effect in NV^- centers,[33] while the static JT seems to contradict the existing data.[31,51]

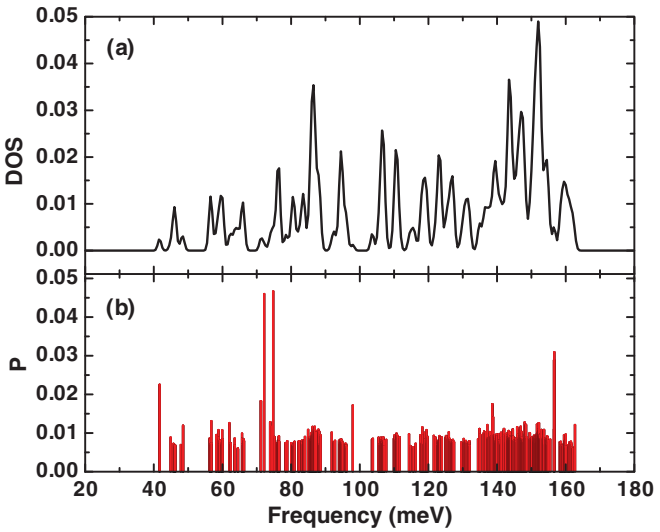

FIG. 3. (Color online) The total density of vibrational states (a) and the IPRs of the corresponding modes (b) for the ground state of the NV^- center. The graph (black solid line) in (a) was smeared, following the standard practice, by convolution of the calculated discrete set of frequencies with the Gaussian line of width 0.5 meV.

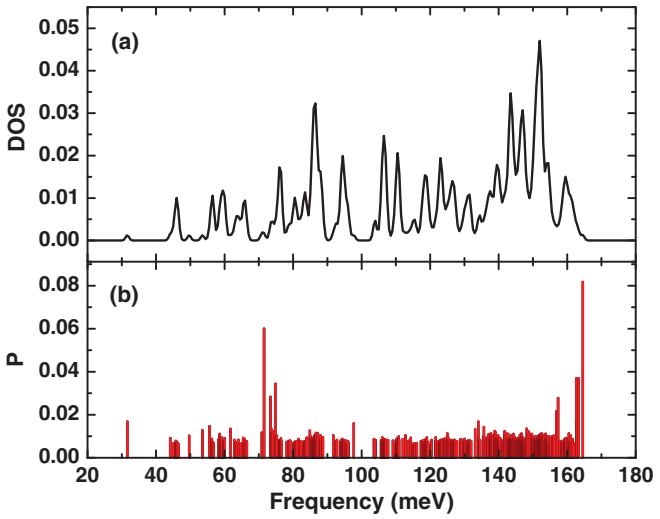

FIG. 4. (Color online) The total density of vibrational states (a) and the IPRs of the corresponding modes (b) for the excited C_{1h} state of the NV^- center. The curve (black solid line) in (a) was smeared, following the standard practice, by convolution of the calculated discrete set of frequencies with the Gaussian line of width 0.5 meV.

Our calculations seem to support the picture of the dynamical JT effect, giving the barrier height E_{JT} of order of 10 meV, and the relevant vibrational frequencies being an order of magnitude larger. This is the indication of the weak-coupling regime, and is in agreement with the known experimental facts (such as, e.g., small renormalization of the g factor, and the shape of the optical transition bands). However, detailed quantitative theory requires a special focused investigations, which would include the lattice nonlinearity and the many-body effects associated with it. Such a study is to be performed in the future. Therefore below we choose the C_{1h} configuration to study the lattice vibrations in the excited state. Fortunately, the results below are not very sensitive to this choice (see Appendix B for more details).

IV. LATTICE VIBRATIONS AND QUASILOCALIZED VIBRATIONAL MODES OF THE NV^- CENTER

When a defect is introduced in a perfect lattice, the localized vibration modes may appear in the phonon spectrum.[53] If the energy of such a mode lies in the gap of the phonon spectrum, or above the highest phonon mode of the perfect lattice, then the vibration amplitude decays exponentially away from the defect (complete localization). But when this mode lies inside the phonon spectrum of the perfect lattice, it can hybridize with the delocalized phonons, and give rise to a quasilocalized vibrational mode (qLVM), which is not completely localized, but whose amplitude still concentrates in the immediate vicinity of the defect. The degree of the mode localization can be quantified by its inverse participation ratio (IPR), defined as

$$P = \sum_{j=1}^{3N} (\mathbf{u}_j \cdot \mathbf{u}_j)^2 \Big[\sum_{j=1}^{3N} \mathbf{u}_j \cdot \mathbf{u}_j \Big]^{-2}, \qquad (1)$$

where N is the number of atoms in the system, and $\mathbf{u}_j$ is the normalized $3N$-dimensional vector of the atomic displacements of the corresponding vibrational eigenmode.[54] IPR characterizes a typical number of atoms involved in a given vibration, so that for completely delocalized phonons $P \sim 1/N$ is almost zero for macroscopic systems, while for completely localized modes P remains finite independently of the system size.

The total density of states (DOS) of the lattice vibrations in the ground state of the NV^- center and the IPRs of the corresponding modes are shown in Fig. 3. The corresponding graphs for the excited orbital state of the C_{1h} symmetry are presented in Fig. 4. In both figures, one can see that a large number of modes with different degrees of localization appears in the diamond lattice with the NV^- center. Particularly prominent are several qLVMs with P as large as 0.03–0.05. Such modes are very strongly localized near the NV^- center, and involve noticeable vibrations of only four to six atoms; the remaining contribution to the value of P is due to very small vibrations of more distant atoms. Note that the distinction between quasilocalized and delocalized modes is gradual. In this paper, we define qLVMs as the vibration modes that have IPRs larger than 0.015 for calculations with a 215-atom supercell (for a smaller supercell, and for comparison with Ref. 39 see Appendix C). In this way, e.g., we identify 8 qLVMs in the ground state, and 12 qLVMs in the excited C_{1h} state. The list of the resulting qLVMs is given in Table I for the ground state and in Table II for the excited C_{1h} state. All modes are infrared active.

Upon the optical excitation, the qLVMs undergo significant changes, as clearly seen from comparison of Figs. 3(b) and 4(b), and Tables I and II. The qLVM with the frequency of 41.66 meV (336 cm^{-1}), which is clearly seen in the ground state, disappears in the excited state, and a new qLVM at 31.62 meV (255 cm^{-1}) appears in the excited state. Also,

TABLE I. Parameters of the quasilocalized vibrational modes with largest IPR in the C_{3v} ground state: frequency ω, IPR P, and symmetry.

ω (meV)	41.66	71.21	72.16	74.79	97.95	138.63	156.64	156.70
P	0.023	0.018	0.046	0.047	0.017	0.017	0.029	0.031
Symmetry	e	e	a	a	a	e	e	a

the group of qLVMs with frequencies slightly above 70 meV undergoes some changes: they become less localized in the excited state. Also, the group of the qLVMs at high frequencies, around 140–160 meV, undergoes noticeable change.

Note that most qLVMs are barely seen in the total DOS, Figs. 3(a) and 4(a), and only the IPR analysis allows us to discern them. To see the changes in the qLVMs in more detail, in Fig. 5 we present the projected DOS (PDOS) corresponding only to the vibrations of the nitrogen and the three carbons adjacent to the vacancy. In the ground state, all carbons are equivalent, and have the same PDOS. In the C_{1h} excited state, one carbon (denoted as C_1) is different from the two others (denoted as C_2 and C_3, and related to each other by reflection in the mirror plane $\{110\}$ passing through N, C_1, and the vacancy site), so that only the PDOS of the C_2 and C_3 atoms are the same. Figure 5 shows, in particular, that both the ground-state qLVM at 41.66 meV and the excited-state qLVM at 31.62 meV are associated almost completely with the carbon vibrations. The qLVM at 41.66 meV is doubly degenerate (e type), so the contributions of different carbons are not well defined, while the excited-state qLVM at 31.62 meV is associated exclusively with C_1 vibrations.

Next, the group of qLVMs slightly above 70 meV, which includes both nitrogen and carbon vibrations, shows moderate changes in the excited state. But the changes in the high-frequency qLVMs, around 140–160 meV, are very noticeable: the modes associated primarily with N vibrations shift toward lower energies, while the carbon vibrational modes acquire higher frequencies. These changes are likely to come from the electron transfer from carbons to the nitrogen (from the $\bar{\nu}$ to the $\bar{e}_x$ orbital, Fig. 2), which accompanies the optical excitation. Filling of the orbitals near carbon atoms makes the bonds stiffer, while the depletion of the nitrogen orbitals makes them softer, with corresponding changes in the qLVM frequencies.

Our calculations provide an even more detailed picture of each relevant qLVM, identifying its type (bond stretching, bond bending, etc.), and visualizing the motion of all atoms. In Figs. 6 and 7, we present the atomic vibration patterns of several important qLVMs for the ground and the excited state, respectively. In particular, the qLVMs with frequencies around 70 meV are shown: these modes are important for discussion of experiments given below. Detailed assessment of several other qLVMs is presented in Appendix A. Here we just mention that

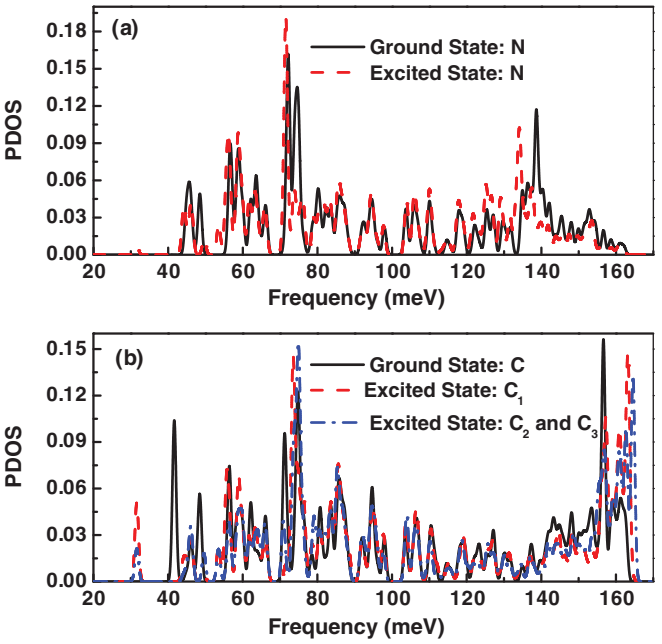

FIG. 5. (Color online) (a) Projected DOS (PDOS) of the vibrations associated with the carbon atoms adjacent to the vacancy. The ground-state PDOS of all carbons are the same (black solid line), while in the excited state the PDOS of the C_1 carbon (dash-dotted green line) is different from the PDOS of the C_2 and C_3 atoms (dashed red line). (b) PDOS of the vibrations associated with the nitrogen atom. The ground-state PDOS is shown with the black solid line, and the excited-state PDOS is shown with the dashed red line. All curves were smeared, following the standard practice, by convolution of the calculated discrete set of frequencies with the Gaussian line of width 0.5 meV.

all the analysis and the ideas presented above are consistent with detailed consideration of qLVMs.

V. COMPARISON WITH THE EXPERIMENTAL RESULTS.

The optical transition between the ground and the excited state is accompanied by the changes in the atomic positions in the neighborhood of the defect site, i.e., involves absorption and emission of the lattice vibration quanta.[27,28] The zero-phonon line (ZPL) in the optical spectrum, which corresponds to the vertical transition (no absorption/emission of the vibrational quanta), is accompanied by sidebands corresponding to absorption/emission of vibration quanta. For NV^- center, the ZPL has the energy 1.945 eV (640 nm), while the vibronically broadened sidebands extend well beyond 750 nm at room temperature. Since the optical transitions are tightly linked to the lattice vibrations, the studies of the optical emission and absorption provide clues about the relevant vibrational modes. In particular, in Ref. 30, the absorption and luminescence spectra have been studied in detail, and the DOS of the vibrations participating in the optical transition has been

TABLE II. Parameters of the quasi-localized vibrational modes with largest IPR in the C_{1h} excited state: frequency ω and IPR P.

ω (meV)	31.62	71.53	73.42	74.82	97.70	134.07	156.85	157.34	162.69	162.77	163.35	164.57
P	0.017	0.060	0.028	0.034	0.016	0.017	0.022	0.028	0.037	0.017	0.037	0.082

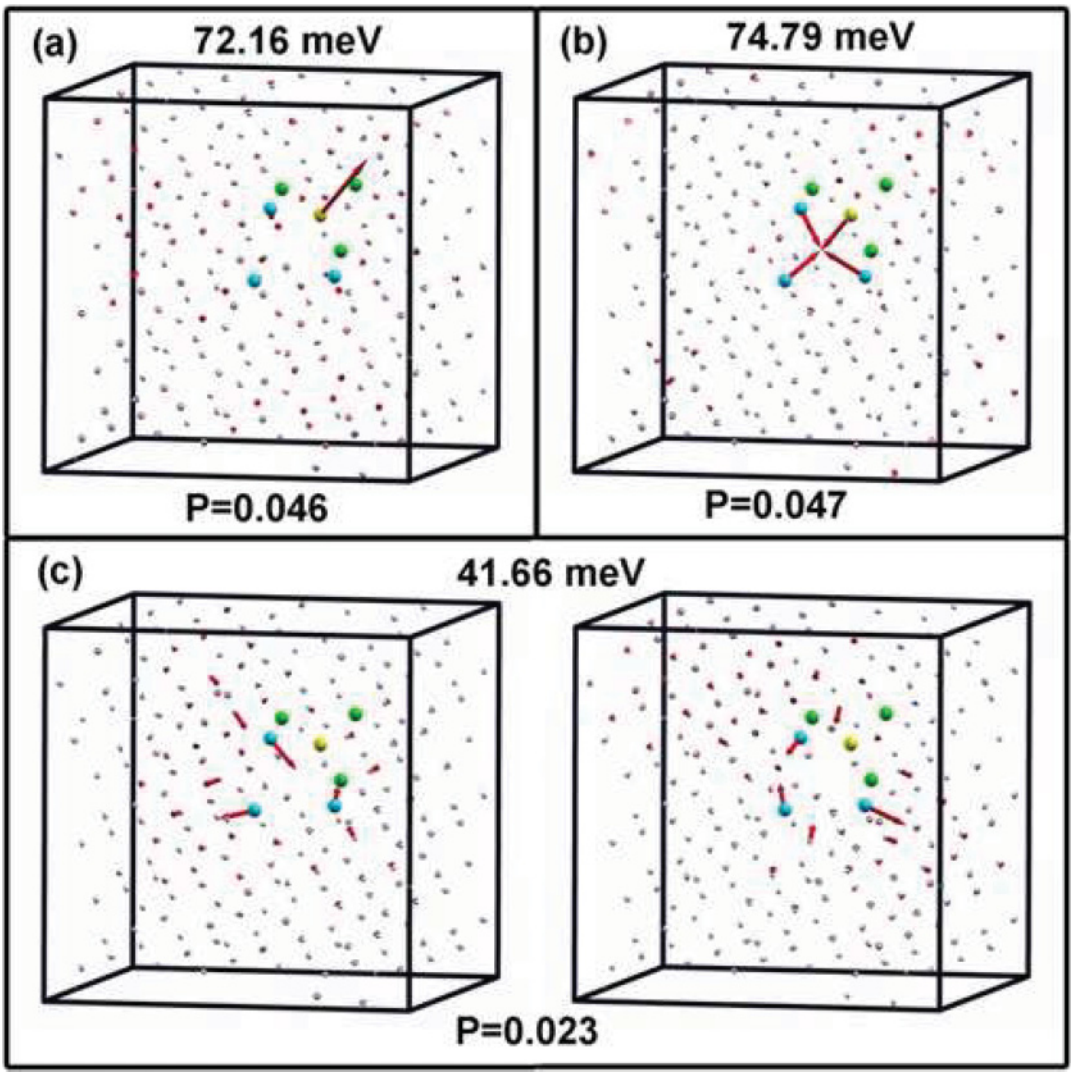

FIG. 6. (Color online) qLVMs in the ground state of the NV^- center: atomic vibration patterns of several modes of different symmetry having largest IPR. The red arrows show the atomic vibrations, the arrow length is proportional to the vibration amplitude of a given atom. (a),(b) Modes of a symmetry, with energies of 72.16 and 74.79 meV; (c) two degenerate modes of e symmetry with the energy of 41.66 meV appearing in the ground state but not in the excited state. Yellow spheres denote N atom, blue spheres denote the C atoms adjacent to the vacancy, green spheres denote the C atoms adjacent to the N atom. Small gray spheres are the other carbon atoms in the diamond lattice.

calculated. It has two broad peaks with maxima around 70 and 140 meV and width of order of 50 meV each; see Fig. 6. Later, more detailed examination of the PL spectra[31] revealed the well-defined one-phonon sidebands, which correspond to a vibration mode of a symmetry with the energy of 70 meV. Moreover, the absorption band was different from the emission band, demonstrating at least two closely spaced peaks.

Our calculations allow a direct comparison with these experimental results. First, let us focus on the DOS $g(\omega)$ calculated from the experimental data in Ref. 30. The qLVMs are expected to play a primary role in optical transition, in comparison with the delocalized phonons, and we expect that the experimentally extracted DOS is associated mostly with qLVMs, as $g(\omega)$ is mostly governed by the vibration amplitude at the defect site.[53] In Fig. 8, we compare the experimentally obtained $g(\omega)$ curve (taken from Ref. 30) with the total vibrational DOS, and with the projected DOS associated only with the vibrations of the nitrogen atom and the three carbons adjacent to the vacancy. For comparison with the experimental data, the discrete lines corresponding to individual modes have been broadened, following the standard practice, by convolution with the Gaussian of the width 10 meV, corresponding to the low resolution of the method used in Ref. 30. The projected DOS practically coincides with the experimental data thus confirming our expectation, while the total DOS demonstrates a serious difference in the positions of the two peaks and in their relative amplitude. Comparing Figs. 8 and 3, we see that the two experimentally found peaks correspond to the two groups of qLVMs, one around 70 meV and the other around 140–160 meV. These results clearly show the crucial influence of the qLVMs on the optical emission and absorption.

In the subsequent work,[31] the influence of vibrations on the emission/absorption has been analyzed in much finer detail,

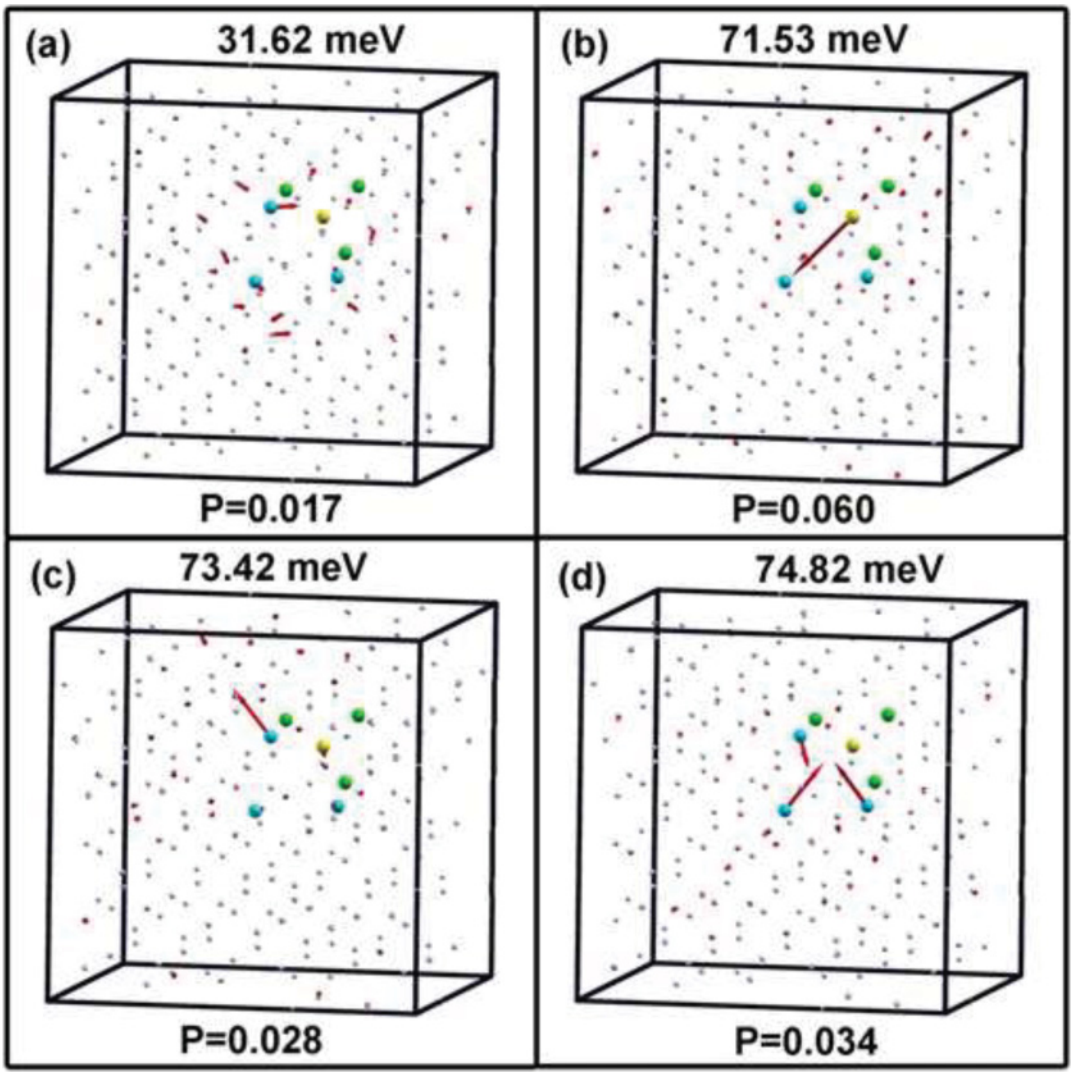

FIG. 7. (Color online) qLVMs in the excited state of the NV^- center: atomic vibration patterns of several modes of different symmetry having largest IPR. The red arrows show the atomic vibrations, the arrow length is proportional to the vibration amplitude of a given atom. (a) Mode of frequency 31.62 meV appearing in the excited state; (b)–(d) modes with frequencies 71.53, 73.42, and 74.82 meV: these are the modes with largest IPR belonging to the group of qLVMs near 70 meV. Yellow spheres denote N atom, blue spheres denote the C atoms adjacent to the vacancy, green spheres denote the C atoms adjacent to the N atom. Small gray spheres are the other carbon atoms in the diamond lattice.

at the level of individual vibronic peaks. It has been found that the vibronic spectra show a clear one-phonon sideband with the vibronic frequency of approximately 70 meV. The experiments have been performed at low temperatures, so that the starting state for both absorption and emission is likely to contain no qLVM quanta, while the final state for absorption (emission) will contain a single quantum of the qLVM corresponding to the excited (ground) state.[27,29] We see immediately that the qLVM group with the frequencies near 70 meV, analyzed above and shown in Figs. 6 and 7, is exactly the right candidate for explanation of this feature. They also have correct a symmetry; see Tables I and II.

A puzzling feature found in Ref. 31 is that the absorption sideband looks like a doublet of two individual lines, with the width of order of 20 meV each, and the peak-to-peak distance of only 3 meV (significant broadening is likely caused by the random stresses in the sample). Note that the multiplet structure of the one-phonon sidebands is fully consistent with our results: we have a group of at least three closely spaced qLVMs near 70 meV in both excited and ground state. The apparently single-peak sideband in emission and doublet in absorption, shown in Fig. 6 of Ref. 31, are equally likely to be made of three peaks of different height, each inhomogeneously broadened by 20 meV. Therefore we do not analyze this feature in more detail. Possibly, future measurements on a single NV^- center, free of such a large inhomogeneous broadening, will convincingly resolve the fine structure of these sidebands.

For a similar reason, we do not discuss the spectral signatures of the ground-state 41.66-meV and the excited-state 31.62-meV qLVMs. One might argue that the steeply rising edge of the one-phonon sideband in Fig. 6 of Ref. 31 does show a shoulder in the right position (near 1.9 eV), but this claim would be way too speculative.

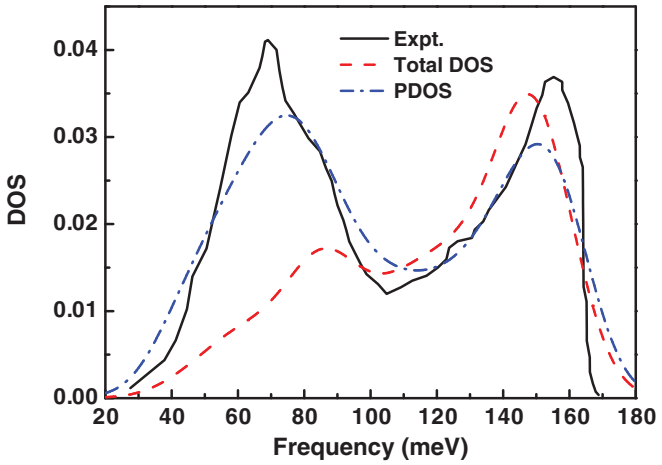

FIG. 8. (Color online) The experimentally determined DOS of the vibrations affecting the optical transition (black solid line) are compared with the calculations results. The blue dash-dotted line denotes the calculated projected DOS of the vibrations associated with the four atoms (nitrogen and three carbons) comprising the core of the NV^- center. The red dashed line denotes the calculated total DOS of the lattice vibrations. An excellent quantitative agreement between the experiments and the calculated projected DOS is clearly visible. Both calculated DOS were smeared by convolution with the Gaussian of the width 10 meV, corresponding to the low resolution of the experimentally determined DOS.

VI. CONCLUSIONS

We have performed detailed first-principles study of the localized distortions and (quasi)localized vibration modes (qLVMs) of NV^- centers in diamond. Our calculations show that the presence of NV^- center gives rise to a large number of qLVMs with different degree of localization.

We found that in the high-symmetry C_{3v} excited state of the NV^- center some qLVMs become unstable, and lead to lowering of the symmetry to C_{1h}. Such a lowering is expected, since the excited state of the NV^- center is a typical example of Jahn-Teller unstable system. Our results seem to support the earlier suggestion[33] that the dynamical Jahn-Teller effect takes place. Our calculations indicate the regime of the weak vibronic coupling, with the mode frequencies about an order of magnitude larger than the Jahn-Teller energy. While the quantitative first-principles theory of this effect for the NV^- center is lacking, it constitutes an exciting topic for future work.

Next, we have analyzed and described some interesting qLVMs in the ground and excited orbital states of the NV^- center, and discussed the changes in the qLVM density of states occurring upon optical excitation. We have performed a comparison of our results with the experimental data reported in Refs. 30 and 31. We have shown that the calculated DOS of the qLVMs is in very good quantitative agreement with the results of Refs. 30, demonstrating two peaks near

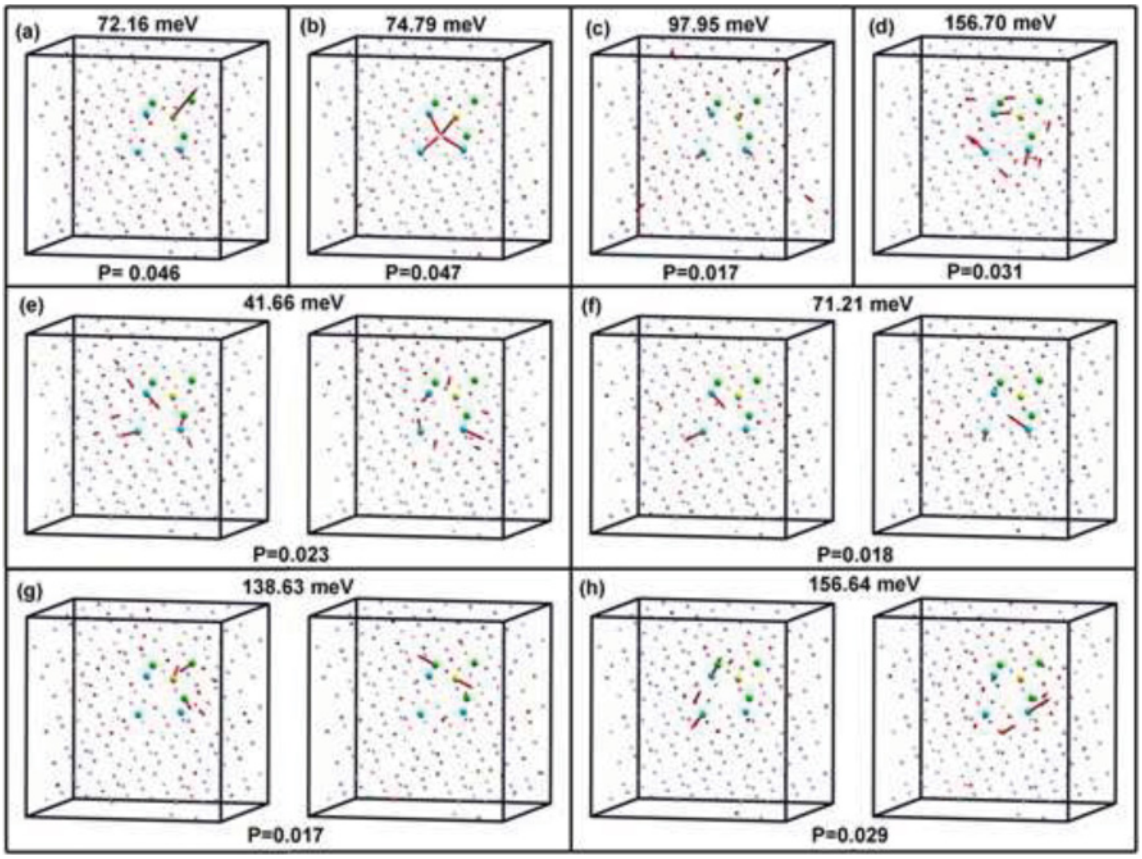

FIG. 9. (Color online) qLVMs in the ground state of the NV^- center: atomic vibration patterns of several modes of different symmetry having largest IPR. Yellow spheres denote N atom, blue spheres denote the C atoms adjacent to the vacancy, green spheres denote the C atoms adjacent to the N atom. Small gray spheres are the other carbon atoms in the diamond lattice.

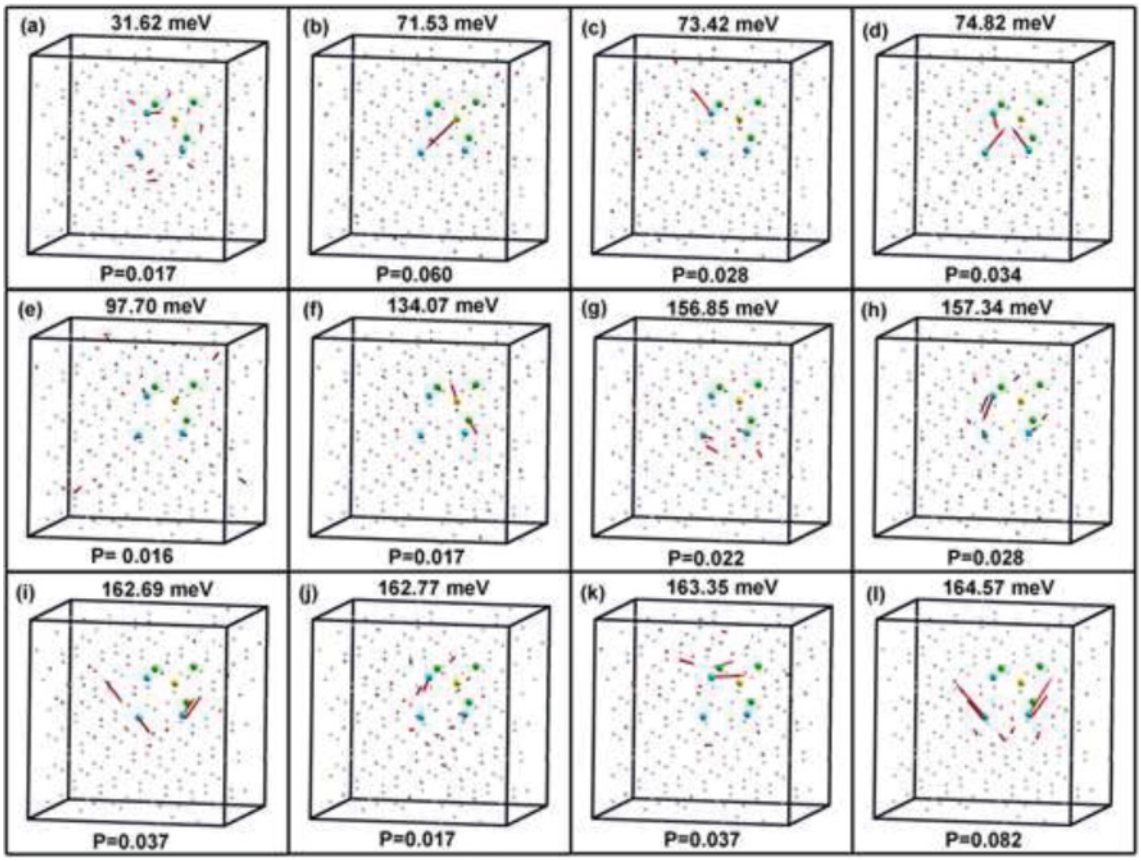

FIG. 10. (Color online) qLVMs in the excited C_{1h} state of the NV^- center: atomic vibration patterns of several modes having largest IPR. Yellow spheres denote N atom, blue spheres denote the C atoms adjacent to the vacancy, green spheres denote the C atoms adjacent to the N atom. Small gray spheres are the other carbon atoms in the diamond lattice.

70 meV and 140–160 meV. These peaks are determined by the corresponding groups of highly localized modes. Therefore, as expected, qLVMs crucially impact the optical properties of the NV^- centers in diamond.

We have also demonstrated that the group of qLVMs with frequencies near 70 meV is likely to explain the features of the one-phonon sideband observed in Ref. 31, possibly including their multiplet structure. However, detailed resolution of this issue requires further experimental and theoretical work, such as high-resolution measurements of the absorption/emission spectrum on a single NV^- center, and highly precise first-principles calculations of the electron-phonon coupling.

ACKNOWLEDGMENTS

We thank R. Hanson, D. D. Awschalom, G. D. Fuchs, A. Gali, and N. Manson for useful discussions on phonon properties of the NV^- centers. This work was performed at the Ames Laboratory of the US Department of Energy, and was supported by the Department of Energy–Basic Energy Sciences, Division of Materials Science and Engineering, under Contract No. DE-AC02-07CH11358. Most calculations have been performed using the computers at the National Energy Research Supercomputing Centre (NERSC) in Berkeley. J.Z. also acknowledges support from the China Scholarship Council (File No. 2009631039).

APPENDIX A: ATOMIC DISPLACEMENT PATTERNS OF SEVERAL GROUND-STATE AND EXCITED-STATE QLVMs

Below, we present the patterns of atomic displacements for several ground-state and excited-state qLVMs having large IPRs.

In the C_{3v} ground state, the lowest-energy localized a mode at 72.16 meV is shown in Fig. 9(a). It is strongly localized on the nitrogen: the N atom moves in the direction perpendicular to the plane defined by the three C atoms around the vacancy. The two a modes shown in Figs. 9(b) and 9(c), with the frequencies 74.79 and 97.95 meV, are the breathing modes of the four first-neighbor atoms of the vacancy: all four atoms move to (or away from) the vacancy. The displacements of the four first neighbor atoms in the 97.95-meV mode are smaller than those in the 73.79 meV mode indicating less localization of the breathing mode at 97.95 meV. The other a mode at 156.7 meV, shown in Fig. 9(d), is a twisting mode around the NV^- center. The first- and second-neighbor carbon atoms from the vacancy rotate in different directions.

The eigenvectors of the four pairs of doubly degenerate e modes, at the frequencies of 41.66, 71.21, 138.63, and 156.64 meV, are shown in Figs. 9(e)–9(h). The two lower-energy localized e modes, Figs. 9(e) and 9(f), are mostly C-N-C angle bending modes. The third one, shown in Fig. 9(g), with a smaller IPR, is the N-C stretching mode at the NV^- center.

The qLVM shown in Fig. 9(h) is a C-C stretching mode: carbon atoms around the vacancy move in the out-of-plane direction, and at the same time, their neighboring carbon atoms move in the opposite direction.

The displacement patterns of the qLVMs in the C_{1h} excited state are shown in Fig. 10, and are quite different from the ground-state qLVMs. There is no doubly degenerate mode in the structure with C_{1h} symmetry. Among the 12 localized modes with largest IPR, only one, with frequency 71.53 meV, shown in Fig. 10(b), is similar to the ground-state mode at 72.16 meV. Six qLVMs at 134.07, 157.34, 162.69, 162.77, 163.35, and 164.57 meV, shown in Figs. 10(f) and 10(h)–10(l), respectively, are the N-C and C-C stretching modes. There are three localized C-N-C angle bending modes at 31.62 meV, Fig. 10(a), at 74.82 meV, Fig. 10(d), and at 156.85 meV, Fig. 10(g). One breathing mode is seen at 97.70 meV, Fig. 10(e), which has smaller IPR. Finally, the mode at 73.42 meV has a C atom moving opposite to the vacancy, as shown in Fig. 10(c). In all the excited-state qLVMs discussed above, the C_1 carbon atom moves independently, while the other two equivalent carbons move collectively to maintain the C_{1h} symmetry. The carbon atoms adjacent to the displaced carbons move in the same plane. This plane is formed by the three first-neighbor carbons in such a way that the rotation and translation of the whole system is absent. Due to the low C_{1h} symmetry, all these modes are IR active.

APPENDIX B: COMPARISON OF THE EXCITED HIGH-SYMMETRY C_{3V} AND LOW-SYMMETRY C_{1h} ORBITAL STATES

As discussed in Sec. III, the high-symmetry C_{3v} excited orbital state of the NV^- center exhibits several modes with large negative frequencies. Moreover, when the geometry optimization for the excited state starts from a lower-symmetry atomic arrangement, the relaxation does not proceed to the high-symmetry C_{3v} configuration: the fully relaxed state has low C_{1h} symmetry. Different choices for the initial low-symmetry arrangements lead to the same fully relaxed C_{1h} configuration (more precisely, to one of the three such configurations, related to each other via rotation by the angle $2\pi/3$ around the symmetry axis of the parent C_{3v} structure). Thus our calculations unequivocally support the presence of the Jahn-Teller (JT) effect in the excited state of the NV^- center. Furthermore, the energy difference between the C_{1h} and C_{3v} configurations is of order of several meV (6.4 meV for a 215-atom supercell and 7.7 meV for a 511-atom supercell), much smaller than the relevant vibrational frequencies (tens to hundreds meV). Along with the existing experimental data,[31,33,51] this suggests the dynamical JT effect, where the total C_{3v} symmetry is a result of zero-point motion between three degenerate minima of C_{1h} symmetry.

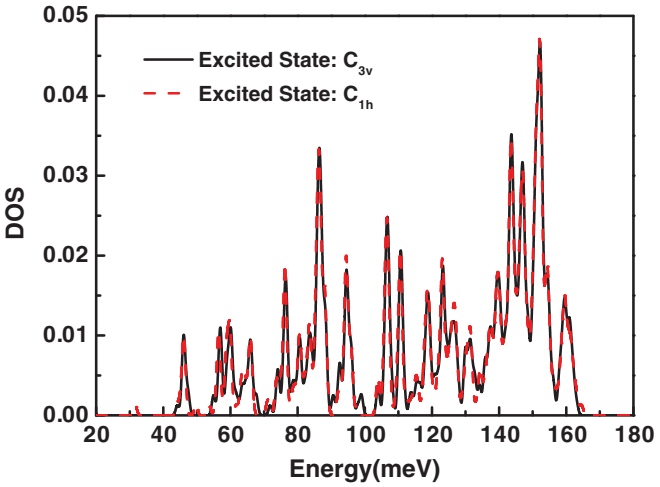

FIG. 11. (Color online) The total density of vibrational states for the high-symmetry C_{3v} (solid black line) and the low-symmetry C_{1h} (dashed red line) configurations for the excited orbital state of the NV^- center. The difference in the density of states for two different configurations is small, and the two curves are very close to each other, except for a small peak at 31.62 meV.

Note, however, that our present calculations have been performed within adiabatic approximation, while a full simulation of the entangled quantum-mechanical motion of atoms and electrons is needed to quantitatively describe the JT effect. Moreover, our results demonstrate that the JT distortion from the C_{3v} to the C_{1h} configuration is accompanied by mixing between different vibrational modes, so that vibrational anharmonicity has to be taken into account for detailed quantitative description of the JT effect in the excited state of the NV^- center. This situation is very different from the simplified cases considered traditionally.[50] Such a study requires a separate full-fledged investigation, and is far beyond the goal of the present work.

For these reasons, in the main text above, we took the C_{1h} configuration as representative for studying the vibrations in the excited state. Fortunately, the results are not very sensitive to this choice. For instance, the densities of vibrational states (DOS) in the C_{1h} and in the C_{3v} configurations are given in Fig. 11. The two curves are very close to each other, except for a small peak at 31.62 meV. Similar results are obtained for projected DOS.

TABLE III. Parameters of the quasilocalized vibrational modes with largest IPR in the C_{3v} ground state: frequency ω, IPR P, and symmetry. Comparison of the results obtained with 215-atom (first and second rows) and 63-atom (third and fourth rows) supercells, and the results of Ref. 39 (fifth row).

ω (meV), 215 atoms	41.66	56.75		71.21	72.16	74.79	97.95	138.63	156.64	156.70
P, 215 atoms	0.023	0.013		0.018	0.046	0.047	0.017	0.017	0.029	0.031
ω (meV), 63 atoms	56.93	58.10	61.72	74.26	74.25	75.77	95.51	137.90	155.46	154.81
P, 63 atoms	0.061	0.057	0.049	0.037	0.079	0.124	0.037	0.055	0.052	0.059
ω (meV), Ref. 39	59.1	59.7	63.3		77.0					
Symmetry	e	a	e	e	a	a	a	e	e	a

TABLE IV. Parameters of the quasi-localized vibrational modes with largest IPR in the C_{1h} excited state: frequency ω, IPR P, and symmetry. Comparison of the results obtained with 215-atom (first and second rows) and 63-atom (third and fourth rows) supercell.

ω (meV), 215 atoms	31.62	71.53	73.42	74.82	97.70	134.07	156.85	157.34	162.69	162.77	163.35	164.57
P	0.017	0.060	0.028	0.034	0.016	0.017	0.022	0.028	0.037	0.017	0.037	0.082
ω (meV), 63 atoms	56.49	73.21	73.86	76.15	94.29	135.91	144.21	151.75	153.70	153.91	160.95	165.51
P	0.093	0.067	0.067	0.111	0.036	0.076	0.050	0.053	0.049	0.052	0.062	0.085

APPENDIX C: COMPARISON OF THE PRESENT CALCULATIONS AND THE CALCULATIONS OF REF. 39

Localized vibrational modes of NV^- center in diamond have been recently studied in Ref. 39. Following the request of the referee, here we provide a brief comparison of the results given in our present work and in Ref. 39. First, our calculations show that for the high-symmetry C_{3v} configuration of the excited orbital state, several vibrational modes are unstable, having large negative frequencies. The configuration corresponding to a local minimum of the total adiabatic potential energy, where all vibrational modes are stable, has lower C_{1h} symmetry. Correspondingly, in our work all excited-state vibrations have been calculated and analyzed for this low-symmetry configuration. Reference 39 does not report unstable modes, and the calculations presented there have been performed for the high-symmetry C_{3v} excited-state configuration.

Second, in our work, the quasilocalized vibrational modes (qLVMs) are analyzed and identified in a systematic way, by calculating the inverse participation ratio (IPR) of every mode. This clearly shows that the distinction between quasilocalized and delocalized modes is gradual. In this paper, we define qLVM as the vibration mode that has IPR larger than 0.015 for calculations with a 215-atom supercell. In this way, e.g., we identify 8 qLVMs in the ground state, and 12 qLVMs in the excited C_{1h} state, while 4 localized modes in the ground state and 4 localized modes in the excited state have been identified in Ref. 39. Third, most of our calculations employ a supercell with 215 atoms, and in some calculations we have used 511-atom supercell. The calculations of Ref. 39 have been performed for 63 atoms. For detailed comparison, we have also performed calculations using a 63-atom supercell; see Tables III and IV. This comparison shows that the characteristics of most qLVMs for 215-atom and 63-atom supercells look similar. The differences are not large, and are expected from qualitative considerations. Indeed, the IPR values for a smaller system (63 atoms) are expected to be larger than the IPRs for a larger one (215 atoms). In the same way, the vibrational frequencies at the lower end of the spectrum are expected to be smaller for a larger system. The modes reported in Ref. 39 for the ground state are close to the modes obtained in our calculations with the 63-atom supercell. The slight difference in the vibration energies might stem from the different exchange-correlation functional used in the two calculations: our calculations employ GGA-PBE functional, while LDA was used in Ref. 39.

Note that an extra qLVM at 58.10 meV obtained for a 63-atom supercell in the C_{3v} ground state corresponds to the mode at 56.75 meV in the 215-atom supercell. The latter has the IPR value slightly below the threshold of 0.015, as one can see from Table III. Another mode of e symmetry at 61.72 meV (63.3 meV in Ref. 39) is quasilocalized in the 63-atom calculations, but becomes much less localized in the 215-atom calculation, and therefore is not shown in Table III.

[1] L. Childress *et al.*, Science **314**, 281 (2006).
[2] R. Hanson, V. V. Dobrovitski, A. E. Feiguin, O. Gywat, and D. D. Awschalom, Science **320**, 352 (2008).
[3] T. Gaebel *et al.*, Nat. Phys. **2**, 408 (2006).
[4] G. Balasubramanian *et al.*, Nat. Mater. **8**, 383 (2009).
[5] A. Gruber, A. Dräbenstedt, C. Tietz, L. Fleury, J. Wrachtrup, and C. von Borczyskowski, Science **276**, 2012 (1997).
[6] F. Jelezko *et al.*, Appl. Phys. Lett. **81**, 2160 (2002).
[7] C. Santori *et al.*, Phys. Rev. Lett. **97**, 247401 (2006).
[8] B. B. Buckley, G. D. Fuchs, L. C. Bassett, and D. D. Awschalom, Science **330**, 1212 (2010).
[9] L. Robledo, H. Bernien, I. van Weperen, and R. Hanson, Phys. Rev. Lett. **105**, 177403 (2010).
[10] F. Jelezko, T. Gaebel, I. Popa, A. Gruber, and J. Wrachtrup, Phys. Rev. Lett **92**, 076401 (2004).
[11] G. D. Fuchs, V. V. Dobrovitski, D. M. Toyli, F. J. Heremans, and D. D. Awschalom, Science **326**, 1520 (2009).
[12] L. Childress, J. M. Taylor, A. S. Sørensen, and M. D. Lukin, Phys. Rev. Lett. **96**, 070504 (2006).
[13] F. Jelezko, T. Gaebel, I. Popa, M. Domhan, A. Gruber, and J. Wrachtrup, Phys. Rev. Lett. **93**, 130501 (2004).
[14] M. V. G. Dutt, L. Childress, L. Jiang, E. Togan, J. Maze, F. Jelezko, A. S. Zibrov, P. R. Hemmer, and M. D. Lukin, Science **316**, 1312 (2007).
[15] J. M. Taylor *et al.*, Nat. Phys. **4**, 810 (2008).
[16] G. Balasubramanian *et al.*, Nature (London) **455**, 648 (2008).
[17] G. de Lange, D. Risté, V. V. Dobrovitski, and R. Hanson, Phys. Rev. Lett. **106**, 080802 (2011).
[18] A. Beveratos, R. Brouri, T. Gacoin, A. Villing, J. P. Poizat, and P. Grangier, Phys. Rev. Lett. **89**, 187901 (2002).
[19] C. Kurtsiefer, S. Mayer, P. Zarda, and H. Weinfurter, Phys. Rev. Lett. **85**, 290 (2000).
[20] T. M. Babinec, B. J. M. Hausmann, M. Khan, Y. A. Zhang, J. R. Maze, P. R. Hemmer, and M. Loncar, Nat. Nano. **5**, 195 (2010).
[21] F. Kaiser, V. Jacques, A. Batalov, P. Siyushev, F. Jelezko, and J. Wrachtrup, e-print arXiv:0906.3426 (to be published).

[22]E. Togan, Y. Chu, A. S. Trifonov, L. Jiang, J. Maze, L. Childress, M. V. G. Dutt, A. S. Sørensen, P. R. Hemmer, A. S. Zibrov, and M. D. Lukin, Nature (London) **466**, 730 (2010).
[23]G. de Lange, Z. H. Wang, D. Risté, V. V. Dobrovitski, and R. Hanson, Science **330**, 60 (2010).
[24]C. A. Ryan, J. S. Hodges, and D. G. Cory, Phys. Rev. Lett. **105**, 200402 (2010).
[25]B. Naydenov, F. Dolde, L. T. Hall, C. Shin, H. Fedder, L. C. L. Hollenberg, F. Jelezko, and J. Wrachtrup, Phys. Rev. B **83**, 081201(R) (2011).
[26]G. D. Fuchs, V. V. Dobrovitski, D. M. Toyli, F. J. Heremans, C. D. Weis, T. Schenkel, and D. D. Awschalom, Nat. Phys. **6**, 668 (2010).
[27]S. I. Pekar, Zh. Eksp. Teor. Fiz. **20**, 510 (1950) (in Russian).
[28]K. Huang and A. Rhys, Proc. R. Soc. London, Ser. A **204**, 406 (1950).
[29]A. P. Nizovtsev, S. Ya. Kilin, C. Tietz, F. Jelezko, and J. Wrachtrup, Physica B **308–310**, 608 (2001).
[30]G. Davies, J. Phys. C **7**, 3797 (1974).
[31]G. Davies and M. F. Hamer, Proc. R. Soc. London, Ser. A **348**, 285 (1976).
[32]A. Batalov, V. Jacques, F. Kaiser, P. Siyushev, P. Neumann, L. J. Rogers, R. L. McMurtrie, N. B. Manson, F. Jelezko, and J. Wrachtrup, Phys. Rev. Lett. **102**, 195506 (2009).
[33]Kai-Mei C. Fu, C. Santori, P. E. Barclay, L. J. Rogers, N. B. Manson, and R. G. Beausoleil, Phys. Rev. Lett. **103**, 256404 (2009).
[34]L. J. Rogers, R. L. McMurtrie, S. Armstrong, M. J. Sellars, and N. B. Manson, New J. Phys. **11**, 063007 (2009).
[35]P. J. Lin-Chung, Phys. Rev. B **50**, 16905 (1994).
[36]M. D. McCluskey, J. Appl. Phys. **87**, 3593 (2000).
[37]S. K. Estreicher, D. West, J. Goss, S. Knack, and J. Weber, Phys. Rev. Lett. **90**, 035504 (2003).
[38]J. E. Lowther, Comput. Mater. Sci. **46**, 520 (2009).
[39]A. Gali, T. Simon, and J. E. Lowther, New J. Phys. **13**, 025016 (2011).
[40]J. P. Perdew, K. Burke, and M. Ernzerhof, Phys. Rev. Lett. **77**, 3865 (1996).
[41]G. Kresse and J. Furthmüller, Phys. Rev. B **54**, 11169 (1996).
[42]D. Alfè, Comput. Phys. Commun. **180**, 2622 (2009).
[43]N. B. Manson, J. P. Harrison, and M. J. Sellars, Phys. Rev. B **74**, 104303 (2006).
[44]A. Gali, M. Fyta, and E. Kaxiras, Phys. Rev. B **77**, 155206 (2008).
[45]M. Łuszczek, R. Lakowski, and P. Horodecki, Physica B **348**, 292 (2004).
[46]J. A. Larsson and P. Delaney, Phys. Rev. B **77**, 165201 (2008).
[47]F. M. Hossain, M. W. Doherty, H. F. Wilson, and L. C. L. Hollenberg, Phys. Rev. Lett. **101**, 226403 (2008).
[48]A. Lenef and S. C. Rand, Phys. Rev. B **53**, 13441 (1996).
[49]Y. Ma, M. Rohlfing, and A. Gali, Phys. Rev. B **81**, 041204 (2010).
[50]I. B. Bersuker and V. Z. Polinger, *Vibronic Interactions in Molecules and Crystals* (Springer-Verlag, Berlin, Heidelberg, 1989).
[51]G. Davies, Rep. Prog. Phys. **44**, 787 (1981).
[52]For ease of comparison with the previous works, we always keep the notations of the parent group, C_{3v}, when describing the excited state. E.g., we denote the orbital excited state as having ^3E symmetry, although the C_{1h} point group has only singlet representations.
[53]A. A. Maradudin, *Solid State Physics*, Vol. 18 (Academic, New York, 1966) p. 273.
[54]C. Z. Wang and K. M. Ho, Phys. Rev. Lett. **71**, 1184 (1993).